ELSEVIER

Engineering Analysis with Boundary Elements 29 (2005) 224–231

ENGINEERING ANALYSIS *with* BOUNDARY ELEMENTS

www.elsevier.com/locate/enganabound

Accuracy of desingularized boundary integral equations for plane exterior potential problems

D.L. Young[a,*], W.S. Hwang[b], C.C. Tsai[a,1], H.L. Lu[a]

[a]*Department of Civil Engineering and Hydrotech Research Institute, National Taiwan University, Taipei 10617, Taiwan, ROC*
[b]*Department of Engineering Science and Ocean Engineering, National Taiwan University, Taipei 10617, Taiwan, ROC*

Received 22 July 2004; revised 4 October 2004; accepted 17 December 2004
Available online 17 March 2005

Abstract

In this article, computational results from boundary integral equations and their normal derivatives for the same test cases are compared. Both kinds of formulations are desingularized on their real boundary. The test cases are chosen as a uniform flow past a circular cylinder for both the Dirichlet and Neumann problems. The results indicate that the desingularized method for the standard boundary integral equation has a much larger convergence speed than the desingularized method for the hypersingular boundary integral equation. When uniform nodes are distributed on a circle, for the standard boundary integral formulation the accuracies in the test cases reach the computer limit of 10^{-15} in the Neumann problems; and $O(N^{-3})$ in the Dirichlet problems. However, for the desingularized hypersingular boundary integral formulation, the convergence speeds drop to only $O(N^{-1})$ in both the Neumann and Dirichlet problems.
© 2005 Elsevier Ltd. All rights reserved.

Keywords: Desingularized boundary integral equation; Desingularized hypersingular boundary integral equation; Potential flows; Normal derivative of boundary integral equation

1. Introduction

Many researchers have intensively investigated the boundary element method (BEM) formulation area, since it can efficiently and conveniently solve the unbounded potential problems. However it is well known that the disadvantage of BEM comes from the singularities inside integral equations. When the matrices of algebraic equations are formed and solved, the existence of singularities may increase the computational load.

There are generally several kinds of methods for overcoming the difficulties of the perplexing singularities, which would be introduced here. One is the direct mathematical integration [1] and the other is the formulation category of desingularized or nonsingular boundary integral equations. An alternative to the direct mathematical integration is the desingularized or non-singular formulation. When the domain of the problem becomes very complex especially for three-dimensional problems, or when high-order elements are adopted in the BEM implementation, the desingularized or non-singular boundary integral equation theory could be a very powerful tool for potential problems compared to the direct mathematical integration.

In the literature, these singularities may be handled at two different stages, before or after the discretization. One method proposed by Hess and Smith [2], is to integrate singularities analytically on a local panel, which takes care of singularities after the discretization. Many researchers later developed diverse numerical schemes to handle singularities on a discretized element. This approach is called the traditional boundary element method or the panel method. Kantorovich and Krylov [3] and Landweber and Macagno [4] proposed another approach to diminish singular integrals before the discretization. Based on known analytic formulas, they used the subtracting and adding back technique to remove singularities in the formulation. Fan and Young [5] applied this method for Stokes flow problems. Webster

* Corresponding author. Tel.: +886 2 2362 6114; fax: +886 2 2362 6114.
E-mail address: dlyoung@ntu.edu.tw (D.L. Young).
[1] Now in Toko University, Chia-Yi County, Taiwan, ROC.

0955-7997/$ - see front matter © 2005 Elsevier Ltd. All rights reserved.
doi:10.1016/j.enganabound.2004.12.007

[6] proposed to move the computing nodes away from the boundary and outside the computational domain, as another way to avoid the singular integrals. This way of moving singular points outside the computational domain is called a desingularized boundary integral method by the works of [7–9]. Although this approach avoids singular integrals, it has the instability of the Fredholm integral equation of the first kind. Therefore for this method to maintain good accuracy, the strategy for choosing the desingularized distance of the fictitious boundary and the mesh size is very important. Another way to circumvent the perplexing singularity proposed by Chen and Tanaka [10] was to introduce the nonsingular general solution instead of singular fundamental solution but to keep source location on the real boundary. They introduced a nonsingular kernel of radial basis functions (RBFs), boundary-type meshfree numerical collocation scheme, to achieve the quite accurate and fast convergent solutions without singularity at all.

The subtracting and adding back technique was used in this paper, to smooth the singularities in the integral equation before the discretization. This kind of approach was modified and referred to as the nonsingular boundary integral method in [5,11], or the desingularized boundary integral method in [12]. The present approach in concept is completely different from the desingularized boundary integral equations in [6–9], which is not to deal with the singularity by putting source off the real boundary. In this study all singular points are located on the boundary, and are regularized by the Gauss' flux theorem and the other theoretical concepts from the potential theory.

As we know any physical problem may have different theoretically equivalent kinds of formulations. For the BEM, it may involve the boundary integral equation or its normal derivative, and both formulations are commonly used. Taking the normal derivative on a boundary integral equation, one will generate a new higher order singularity, which is called the hypersingularity. Recently the normal derivative of boundary integral equations has been very popular, and Hwang [13] and Yang [14] studied its nonsingular formulation. However the discussion of convergence from such kinds of integral equations has been unmentioned. In this paper, the convergence and accuracy of both singular and hypersingular boundary integral equations for the exterior problems are emphasized in a plane problem.

For Neumann problems, the original integral equation is a Fredholm integral equation of the second kind with a regular kernel in a plane case. By taking its normal derivative on it for the same problem, it becomes a hypersingular integral equation. It is a first-kind equation in classification. The original integral equation for the Dirichlet problems is a Fredholm integral equation of the first kind. It turns out to be a second-kind equation after taking the normal derivative. If the kernel of a Fredholm integral equation of the first kind is continuous, after the equation is discretized, an ill-conditioned and non-diagonal dominant matrix occurs. However if the kernel is singular, the resultant matrix may be still diagonal dominant, and stable when the matrix is inverted. In general, the Fredholm integral equation of the second-kind equation with continuous kernel is more suitable than the first-kind equation. However that may not be true if the kernels of these equations are not continuous. The accuracy of each formulation is compared and discussed in the present paper.

2. Formulations of boundary integral equations

Both velocity potentials and stream functions of flow fields satisfy the Laplace equation for a plane potential flow. Let ϕ represent the velocity potential and ψ represent the stream function, and then

$$\nabla^2\phi = \frac{\partial^2\phi}{\partial x^2} + \frac{\partial^2\phi}{\partial y^2} = 0, \tag{2.1}$$

$$\nabla^2\psi = 0 \tag{2.2}$$

As for the boundary conditions, both the velocity potential and the stream function usually satisfy the impermeable condition. Then the boundary condition for the velocity potential can be written as

$$\nabla\phi \cdot \vec{n} = \frac{\partial\phi}{\partial n} = 0, \tag{2.3}$$

where $\vec{n}$ means the outward unit normal vector of the surface Γ as shown in Fig. 1. This type of problem is called the Neumann problem. On the other hand, if a stream function is used, the stream function on the boundary is specified as a constant, such as

$$\psi = C. \tag{2.4}$$

This is called the Dirichlet problem, and usually the constant C is taken as zero without loss of generality.

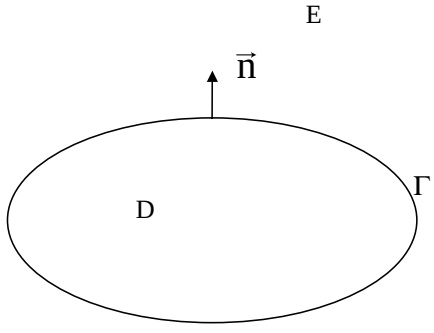

Fig. 1. Interior domain D, exterior region E, boundary Γ and normal vector $\vec{n}$.

If an integral formulation is adopted for an exterior flow, then it can be expressed as follows:

$$(1-\varepsilon(\vec{x}))A(\vec{x}) = -\int_{\Gamma}\left[A(\vec{x}')\frac{\partial G(\vec{x},\vec{x}')}{\partial n_{\vec{x}'}} - G(\vec{x},\vec{x}')\frac{\partial A(\vec{x}')}{\partial n_{\vec{x}'}}\right]\mathrm{d}s + A_I(\vec{x}), \tag{2.5}$$

where A may represent ϕ or ψ, A_I represents an incident flow, and $G(\vec{x},\vec{x}')$ represents the Green's function. In the two-dimensional case, the Green's function can be written as

$$G(\vec{x},\vec{x}') = \frac{1}{2\pi}\ln r, \tag{2.6}$$

where r represents the distances between the field point $\vec{x}$ and the field point $\vec{x}'$. The free-term coefficient is defined as,

$$\varepsilon(\vec{x}) = \int_{\Gamma}\frac{\partial G(\vec{x},\vec{x}')}{\partial n_{\vec{x}'}}\mathrm{d}s \tag{2.7}$$

The coefficient $\varepsilon(\vec{x})$ is equal to 1 when $\vec{x}$ is inside the domain, 1/2 when $\vec{x}$ is on the smooth part of the boundary surface, and 0 when $\vec{x}$ is outside the domain.

2.1. Neumann problems

In this case, the total velocity potential ϕ in the exterior region E replaces A in Eq. (2.5). After applying the impermeable condition to Eq. (2.5), the resultant equation becomes:

$$(1-\varepsilon(\vec{x}))\varphi(\vec{x}) + \int_{\Gamma}\varphi(\vec{x}')\frac{\partial G(\vec{x},\vec{x}')}{\partial n_{\vec{x}'}}\mathrm{d}s = \varphi_\mathrm{I}(\vec{x}) \tag{2.8}$$

where ϕ_I is the incident velocity potential. This is the Fredholm integral equation of the second kind. Substituting Eq. (2.7) into (2.8), one obtains the nonsingular boundary integral equation such as:

$$\phi(\vec{x}) + \int_{\Gamma}\left\{[\phi(\vec{x}') - \phi(\vec{x})]\frac{\partial G(\vec{x},\vec{x}')}{\partial n_{\vec{x}'}}\right\}\mathrm{d}s = \phi_\mathrm{I}(\vec{x}). \tag{2.9}$$

The above equation is used to solve the velocity potential $\phi(\vec{x})$ on the boundary Γ. When $\vec{x}'$approaches $\vec{x}$, in this modified formulation the numerical singularity even no longer exists. The limiting value of the integrand in Eq. (2.9) is zero.

In order to simplify the numerical process, collocation and integration points are put together at the same location when Eq. (2.9) is solved. For accuracy, collocation points are distributed on locations that may generate the most accurate numerical results for the integration in Eq. (2.9). Then a set of algebraic equations is formed as:

$$\sum_{j=1}^{N}(A_{ij}\phi_j) = \phi_{\mathrm{I}i}, \quad i = 1,\ldots,N \tag{2.10}$$

where N is the total number of nodes, ϕ_j denotes $\phi(\vec{x})$ at the jth point, $\phi_{\mathrm{I}i}$ denotes $\phi_\mathrm{I}(\vec{x})$ at the ith point. A_{ij} can be expressed as:

$$A_{ij} = \begin{cases} -\dfrac{1}{2\pi}\dfrac{(\vec{r}_{ij}.\vec{n}_j)}{r_{ij}^2}w_j & j \neq i \\ 1 + \dfrac{1}{2\pi}\displaystyle\sum_{k=1,k\neq i}^{N}\frac{(\vec{r}_{ik}.\vec{n}_k)}{r_{ik}^2}w_k & j = i \end{cases} \tag{2.11}$$

where $\vec{r}_{ij}$ is the vector from the ith node to the jth node, r_{ij} is the distance between the ith and the jth nodes, and w_j denotes the weighting factor at the jth node according to the chosen quadrature rule.

2.2. Dirichlet problems

When $\psi = 0$ is specified on the boundary, and A is replaced by ψ in Eq. (2.5), it becomes the Fredholm integral equation of the first kind.

$$\int_{\Gamma}\frac{\partial\psi(\vec{x}')}{\partial n_{\vec{x}'}}G(\vec{x},\vec{x}')\mathrm{d}s = -\psi_\mathrm{I}(\vec{x}) \tag{2.12}$$

where ψ_I is the undisturbed stream function. To desingularize Eq. (2.12), one needs an auxiliary function to complete the subtracting and adding back technique such as:

$$\int_{\Gamma}\left[\frac{\partial\psi(\vec{x}')}{\partial n_{\vec{x}'}} - \frac{\partial\psi(\vec{x})}{\partial n_{\vec{x}}}\frac{\sigma(\vec{x}')}{\sigma(\vec{x})}\right]G(\vec{x},\vec{x}')\mathrm{d}s + \frac{\partial\psi(\vec{x})}{\partial n_{\vec{x}}}\frac{\phi_\mathrm{e}}{\sigma(\vec{x})} = -\psi_\mathrm{I}(\vec{x}) \tag{2.13}$$

$$\phi_\mathrm{e} = \int_{\Gamma}\sigma(\vec{x}')G(\vec{x},\vec{x}')\mathrm{d}s \tag{2.14}$$

where σ denotes a distribution of source function on the boundary to make the field equipotential in the interior domain, and ϕ_e is the value of the equipotential. Details on this source function can be found in [4] and [11].

Again, Eq. (2.13) becomes a nonsingular boundary integral equation after desingularized process. The numerical implementation of Eq. (2.13) can be expressed as a matrix form:

$$\sum_{j=1}^{N}(B_{ij}\psi_{nj}) = -\psi_{\mathrm{I}i} \quad i = 1,\ldots,N, \tag{2.15}$$

$$B_{ij} = \begin{cases} \dfrac{1}{2\pi}\ln r_{ij}\bullet w_j & j \neq i \\ \dfrac{\phi_\mathrm{e}}{\sigma_i} - \displaystyle\sum_{k=1,k\neq i}^{N}\frac{\sigma_k}{2\pi\sigma_i}\ln r_{ik}\bullet w_k & j = i \end{cases} \tag{2.16}$$

where ψ_{nj} denotes $\partial\psi(\vec{x}')/\partial n$ at the jth point, $\psi_{\mathrm{I}i}$ denotes $\psi_\mathrm{I}(\vec{x})$ at the ith point, and σ_i denotes the source function σ at the ith point.

Table 1
Comparison between the results of the direct mathematical integration and the desingularized theory

Number of nodes	$\int \frac{\partial G}{\partial n} ds$ by desingularized theory	Exact solution of $\int \frac{\partial G}{\partial n} ds$	Error	$\int G\, ds$ by desingularized theory	Exact solution of $\int G\, ds$	Error
16	4.999864×10^{-1}	5.000000×10^{-1}	1.360000×10^{-5}	2.358439×10^{-1}	2.410871×10^{-1}	5.243200×10^{-3}
32	4.999883×10^{-1}	5.000000×10^{-1}	1.170000×10^{-5}	1.626223×10^{-1}	1.640777×10^{-1}	1.455400×10^{-3}
48	4.999915×10^{-1}	5.000000×10^{-1}	8.500000×10^{-6}	1.256592×10^{-1}	1.263280×10^{-1}	6.688000×10^{-4}
64	4.999934×10^{-1}	5.000000×10^{-1}	6.600000×10^{-6}	1.033698×10^{-1}	1.037523×10^{-1}	3.825000×10^{-4}
80	4.999947×10^{-1}	5.000000×10^{-1}	5.300000×10^{-6}	8.834017×10^{-2}	8.858739×10^{-2}	2.472200×10^{-4}

2.3. Examples

The singularity issue is the only difference between the traditional BEM and proposed desingularized BEM formulations. Thus before performing the test examples, the singular integration values obtained by the direct mathematical integration [1] and proposed desingularized theory will be compared. Table 1 describes the comparisons for the uniform distributed constant element in a circle with radius 2. The results show generally good agreement between the direct mathematical integration and the current desingularized theory.

The trapezoidal rule is well known as a very accurate quadrature formula for periodic functions. The problems discussed here are all continuous along the boundary, so the boundary data are all periodic in this sense. Therefore, the trapezoidal rule is chosen as the only numerical integration rule in the following examples.

The test case is chosen as a uniform flow past a circular cylinder. The analytical solution of the velocity potential in the cylindrical coordinates can be expressed as

$$\phi = Ur\left(1 + \frac{a^2}{r^2}\right)\cos\theta \tag{2.17}$$

where a denotes the radius of the circular cylinder, r denotes the distance from the center of the cylinder, U denotes the velocity of the incoming flow, and ϕ is the polar angle from the x-axis. The corresponding incoming flow, ϕ_{I}, is

$$\phi_{\mathrm{I}} = Ux. \tag{2.18}$$

When the same case is tested as a Dirichlet problem, the analytical solution of the stream function is described in a different form:

$$\psi = Ur\left(1 - \frac{a^2}{r^2}\right)\sin\theta \tag{2.19}$$

The stream function of the incoming flow, ψ_{I}, can be expressed as:

$$\psi_{\mathrm{I}} = Uy \tag{2.20}$$

The numerical error is defined by the E_2 norm:

$$E_2 = \sqrt{\frac{1}{N}\sum_{i=1}^{N}(\phi_i^{\text{analytical}} - \phi_i^{\text{numerical}})^2}. \tag{2.21}$$

After calculation, Fig. 2 shows the relative errors for both cases. The nodes are numbered counterclockwise from $\theta = 0$. It is noteworthy that the relative error distributions are uniform along the circle except those points whose exact solutions are zero. Fig. 3 shows the error variation versus the number of mesh nodes for the Neumann problem. For any convex geometry, since $\vec{r}_{ij}\cdot\vec{n}_j$ in Eq. (2.11) is always negative, when $i \neq j$. The summation of off-diagonal terms is less than 1/2 from Gauss' flux theorem. Then the diagonal term in Eq. (2.11) is always greater than 1/2, so the matrix A is a diagonally dominant matrix. It was shown in [11] that the errors decay exponentially with the number of nodes for an ellipse. In this particular case, the accuracy has reached the limit of computer, 10^{-15}, in the test range. The trend of errors is growing with the number of nodes as shown in Fig. 3. This indicates that the error mainly comes from the numerical accumulation, and the discretization error almost disappears. Compared with Eq. (2.10), the property of Eq. (2.15) is not so clear. However Saranen [15] theoretically proved with a different regularization scheme, that for a smooth curve the convergence speed of this integral equation is $O(N^{-3})$. Fig. 4 also confirms this result for the Dirichlet problem in the present scheme.

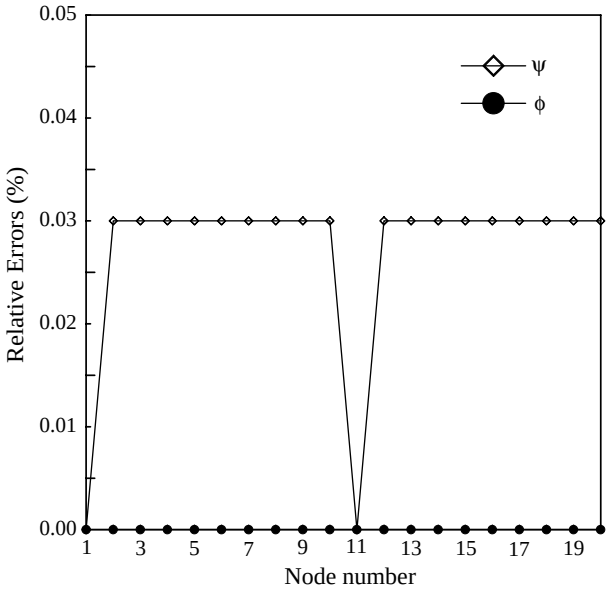

Fig. 2. Relative errors for the velocity potential (ϕ) and the stream function (ψ) of a uniform flow past a circular cylinder by the boundary integral equation.

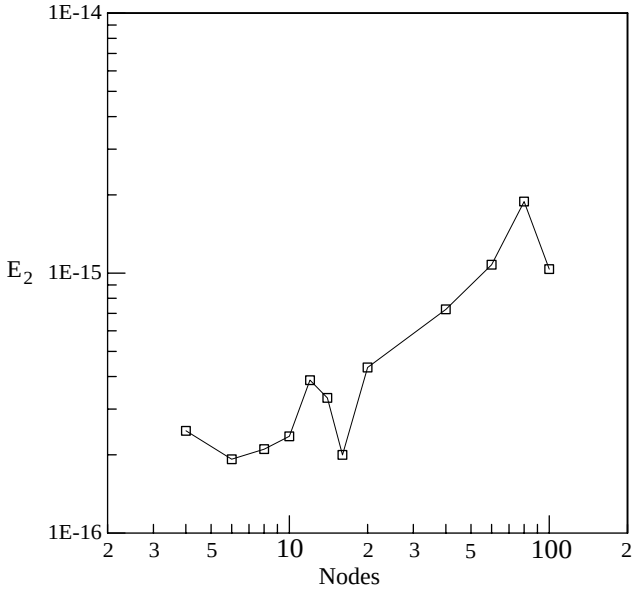

Fig. 3. Root-mean-square errors of the Neumann problem by the boundary integral equation.

3. Formulations of the normal derivative of the boundary integral equations

From the last section we know the original representation of the Dirichlet problem belongs to the first-kind equation. It becomes the second-kind equation after taking its normal derivative.

3.1. Neumann problems

By taking the normal derivative on Eq. (2.5) with respect to $\vec{x}$, and applying the boundary condition of Eq. (2.3), it then yields

$$\frac{\partial \phi_1(\vec{x})}{\partial n_{\vec{x}}} = \frac{\partial}{\partial n_{\vec{x}}} \int_\Gamma \left[\phi(\vec{x}') \frac{\partial G(\vec{x},\vec{x}')}{\partial n_{\vec{x}'}} \right] \mathrm{d}s \tag{3.1}$$

Some further operations are needed, to reasonably simplify the operator in the right-hand side of Eq. (3.1), which details can be found in [13,14,16]. When $\vec{x}$ is on the boundary Γ, the equation becomes hypersingular:

$$\frac{\partial \phi_1(\vec{x})}{\partial n_{\vec{x}}} = \int_\Gamma [\phi(\vec{x}') - \phi(\vec{x})] \frac{\partial^2 G(\vec{x},\vec{x}')}{\partial n_{\vec{x}} \partial n_{\vec{x}'}} \mathrm{d}s \tag{3.2}$$

Note that the original boundary integral equation for the Neumann problems is a Fredholm integral equation of the second kind. However after taking the normal derivative, Eq. (3.2) contains a hypersingular kernel, even though the total integrand is still strongly singular. When the Hadamard finite part is applied to Eq. (3.2), it belongs to the Fredholm integral equation of the first kind [17].

Eq. (3.2) is very difficult to compute. Therefore, as noted below some researchers instead of directly solving the hypersingular equation, proposed a viable approach to solve an associate internal problem. It is seen that there are two integral equations with weakly singular kernels to solve. However these two integral equations can be regularized and both of them belong to the Fredholm integral equation of the second kind. Detailed descriptions can be found in [13,14,16,18,19], and a brief introduction is as follows. Let ζ be the solution of the Laplace equation for the interior region with the boundary condition $\zeta = \phi$ on Γ, then on the boundary

$$\frac{1}{2}\zeta(\vec{x}) = \int_\Gamma \left[\zeta(\vec{x}') \frac{\partial G(\vec{x},\vec{x}')}{\partial n_{\vec{x}'}} - G(\vec{x},\vec{x}') \frac{\partial \zeta(\vec{x}')}{\partial n_{\vec{x}'}} \right] \mathrm{d}s \tag{3.3}$$

Now Eq. (3.3) becomes a Fredholm integral equation of the second kind. To obtain a nonsingular form for Eq. (3.3), one can apply a procedure similar to the treatment of Eqs. (2.5) and (2.9), and obtain

$$\int_\Gamma [\zeta(\vec{x}') - \zeta(\vec{x})] \frac{\partial G(\vec{x},\vec{x}')}{\partial n_{\vec{x}'}} \mathrm{d}s = \int_\Gamma \left[\frac{\partial \zeta(\vec{x}')}{\partial n_{\vec{x}'}} - \frac{\zeta(\vec{x})}{\partial n_{\vec{x}}} \frac{\sigma(\vec{x}')}{\sigma(\vec{x})} \right] G(\vec{x},\vec{x}') \, \mathrm{d}s + \frac{\zeta(\vec{x})}{\partial n_{\vec{x}}} \frac{\phi_e}{\sigma(\vec{x})} \tag{3.4}$$

In the above equation, both ζ and $\partial\zeta/\partial n$ are unknowns. We must solve $\partial\zeta/\partial n$ in advance. If we take the normal derivative on Eq. (3.3), approach ζ to the boundary, and rearrange it we then have:

$$\frac{\partial}{\partial n_{\vec{x}}} \int_\Gamma \zeta(\vec{x}') \frac{\partial G(\vec{x},\vec{x}')}{\partial n_{\vec{x}'}} \mathrm{d}s = \int_\Gamma \frac{\partial G(\vec{x},\vec{x}')}{\partial n_{\vec{x}}} \frac{\partial \zeta(\vec{x}')}{\partial n_{\vec{x}'}} \mathrm{d}s + \frac{1}{2} \frac{\partial \zeta(\vec{x})}{\partial n_{\vec{x}}}. \tag{3.5}$$

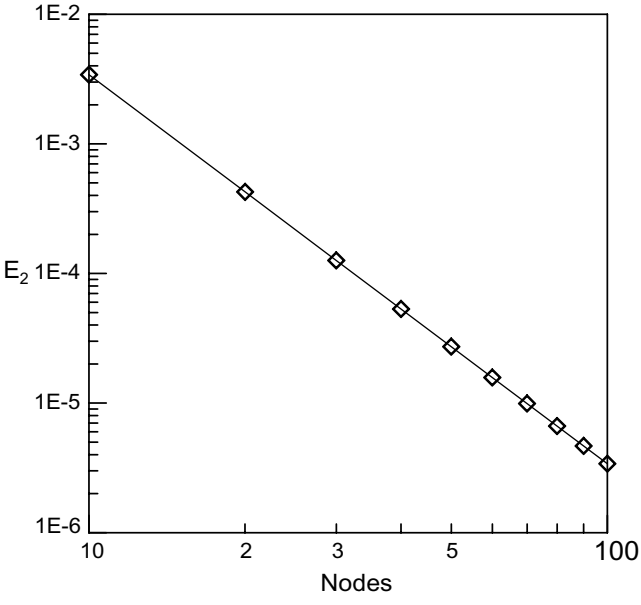

Fig. 4. Root-mean-square errors of the Dirichlet problem by the boundary integral equation.

By combining Eqs. (3.1) and (3.5), and performing some operations, we can get a nonsingular integral formulation [13,14,16,18,19].

$$\frac{\partial \phi_{\mathrm{I}}(\vec{x})}{\partial n_{\vec{x}}} = \int_{\Gamma} \left[\frac{\partial G(\vec{x},\vec{x}')}{\partial n_{\vec{x}}} \frac{\partial \zeta(\vec{x}')}{\partial n_{\vec{x}'}} - \frac{\partial G(\vec{x},\vec{x}')}{\partial n_{\vec{x}'}} \frac{\partial \zeta(\vec{x})}{\partial n_{\vec{x}}} \right] \mathrm{d}s + \frac{\partial \zeta(\vec{x})}{\partial n_{\vec{x}}} \tag{3.6}$$

Eq. (3.6) is used to compute the unknown $\partial\zeta/\partial n$ on the boundary. After $\partial\zeta/\partial n$ is solved, Eq. (3.4) is used to find the unknown ζ on the boundary. Since $\zeta=\phi$ on the boundary, the velocity potential ϕ is obtained for the Neumann problem.

The numerical implementation is similar to the earlier section such as:

$$\sum_{j=1}^{N} (C_{ij}\zeta_{nj}) = \phi_{\mathrm{I}ni}, \quad i = 1, \ldots, N \tag{3.7}$$

where $\phi_{\mathrm{I}ni}$ denotes $\partial\phi_I/\partial n_{\vec{x}}$ at the ith boundary node, ζ_{nj} denotes $\partial\zeta/\partial$n at the jth boundary node, and

$$C_{ij} = \begin{cases} \dfrac{1}{2\pi} \dfrac{(\vec{r}_{ij}.\vec{n}_j)}{r_{ij}^2} w_j & j \neq i \\ 1 + \dfrac{1}{2\pi} \displaystyle\sum_{k=1,k\neq i}^{N} \dfrac{(\vec{r}_{ik}.\vec{n}_k)}{r_{ik}^2} w_k & j = i \end{cases} \tag{3.8}$$

After $\partial\zeta/\partial n$ in Eq. (3.6) are solved, Eq. (3.4) can be discretized such as:

$$\sum_{j=1}^{N} D_{ij}\zeta_j = \sum_{j=1}^{N} B_{ij}\zeta_{nj}, \quad i = 1, \ldots, N \tag{3.9}$$

where B_{ij} is defined in Eq. (2.16), and D_{ij} can be expressed as:

$$D_{ij} = \begin{cases} -\dfrac{1}{2\pi} \dfrac{(\vec{r}_{ij}.\vec{n}_j)}{r_{ij}^2} w_j & j \neq i \\ \dfrac{1}{2\pi} \displaystyle\sum_{k=1,k\neq i}^{N} \dfrac{(\vec{r}_{ik}.\vec{n}_k)}{r_{ik}^2} w_k & j = i \end{cases} \tag{3.10}$$

The difference between A_{ij} and D_{ij} is only when $i=j$, and in fact $D_{ii}=1-A_{ii}$. Since $\partial\zeta/\partial n$ is already solved at nodes by using Eq. (3.7), the unknown ζ on the boundary Γ can be obtained directly from Eq. (3.9).

3.2. Dirichlet problems

The boundary integral equation for the stream function is given in Eq. (2.12), and it is a Fredholm first-kind equation. After taking a differentiation in the normal direction at the point $\vec{x}(x, y)$ and letting it approach to the boundary, the new formulation becomes a Fredholm integral equation of the second kind such as:

$$\frac{1}{2} \frac{\partial \psi(\vec{x})}{\partial n_{\vec{x}}} = \int_{\Gamma} \frac{\partial G(\vec{x},\vec{x}')}{\partial n_{\vec{x}}} \frac{\partial \psi(\vec{x}')}{\partial n_{\vec{x}'}} \mathrm{d}s + \frac{\partial \psi_{\mathrm{I}}(\vec{x})}{\partial n_{\vec{x}}} \tag{3.11}$$

The kernel of the normal derivative of the Green's function is regular in two dimensions, and actually its limiting value is related to the curvature of boundary at that point. However, in order to simplify the calculation, the Gauss' flux theorem is applied to Eq. (3.11) again. Then the integral equation becomes:

$$\int_{\Gamma} \left[\frac{\partial G(\vec{x},\vec{x}')}{\partial n_{\vec{x}'}} \frac{\partial \psi(\vec{x})}{\partial n_{\vec{x}}} - \frac{\partial G(\vec{x},\vec{x}')}{\partial n_{\vec{x}}} \frac{\partial \psi(\vec{x}')}{\partial n_{\vec{x}'}} \right] \mathrm{d}s = \frac{\partial \psi_{\mathrm{I}}(\vec{x})}{\partial n_{\vec{x}}} \tag{3.12}$$

Eq. (3.12) is then totally nonsingular, and its numerical discretization becomes very easy to execute. The unknowns, ψ_n, at nodes on the boundary Γ can be solved through the following equations:

$$\sum_{j=1}^{N} (E_{ij}\psi_{nj}) = \psi_{\mathrm{I}ni} \tag{3.13}$$

where ψ_{nj} denotes $\partial\psi(\vec{x})/\partial n_{\vec{x}}$ at the jth boundary point, and $\psi_{\mathrm{I}ni}$ denotes $\partial\psi_{\mathrm{I}}(\vec{x})/\partial n_{\vec{x}}$ at the ith boundary point. Then, E_{ij} can be expressed as

$$E_{ij} = \begin{cases} -\dfrac{1}{2\pi} \dfrac{(\vec{r}_{ij}.\vec{n}_j)}{r_{ij}^2} w_j & j \neq i \\ -\dfrac{1}{2\pi} \displaystyle\sum_{k=1,k\neq i}^{N} \dfrac{(\vec{r}_{ik}.\vec{n}_k)}{r_{ik}^2} w_k & j = i \end{cases} \tag{3.14}$$

By comparison with Eq. (3.10), we have $E_{ii}=-D_{ii}$.

3.3. Examples

To test the normal derivative of the boundary integral equation, the same previous cases are applied. Eq. (2.17) shows the analytical solution of the velocity potential, and the right-hand side values of equation (3.7) are

$$\phi_{\mathrm{I}ni} = U\cos\theta \tag{3.15}$$

For the Dirichlet case, the analytical solution of the stream function is shown in Eq. (2.19). The values on the right-hand side of Eq. (3.13) are

$$\psi_{\mathrm{I}ni} = U\sin\theta \tag{3.16}$$

Fig. 5 shows the relative errors of the test case with 20 nodes for both the Neumann and Dirichlet conditions. The relative errors in Fig. 5 are uniform for both cases, just like those in Fig. 2. However unlike the last section result, the accuracy of the present formulation seems much worse than that of the boundary integral formulation, as shown in Fig. 2. An interesting feature is shown in Fig. 6, where the trend of the two curves is almost coincident when the number of nodes is large enough. This means

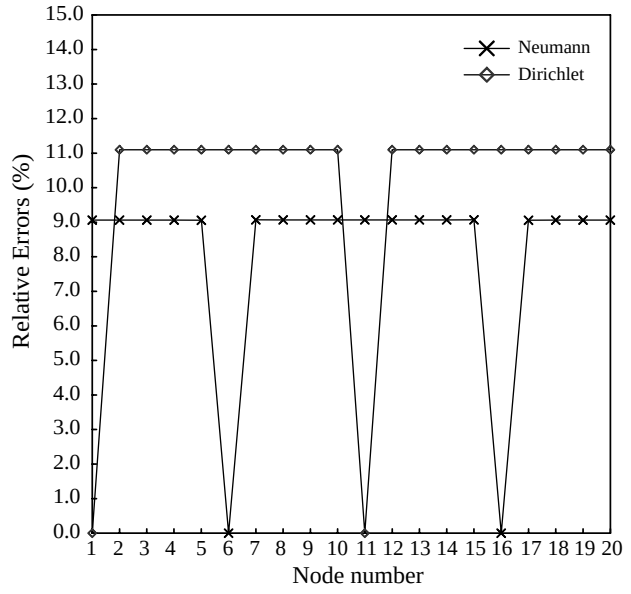

Fig. 5. Relative errors of the normal derivative of velocity potential (Neumann) and the stream function (Dirichlet) of a uniform flow past a circular cylinder.

the convergence speeds are almost the same for both cases. If these two cases are carefully examined, in this special case the elements of matrices D and E have the same values for $i \neq j$, and $D_{ii} = -E_{ii}$. In the test case, D_{ij} and E_{ij} have the same sign for all $i \neq j$, so the sum of absolute values of off-diagonal terms is equal to the absolute value of the diagonal term as shown in Eq. (3.10). Therefore, matrices D and E are not diagonally dominant in general. Nevertheless, Eqs. (3.9) and (3.13) look very similar. Fig. 6 indicates that when N is large enough the root-mean-square errors of both cases have the same order of $O(N^{-1})$. If N is not large, the Neumann problem results are only a little better than the Dirichlet problem results.

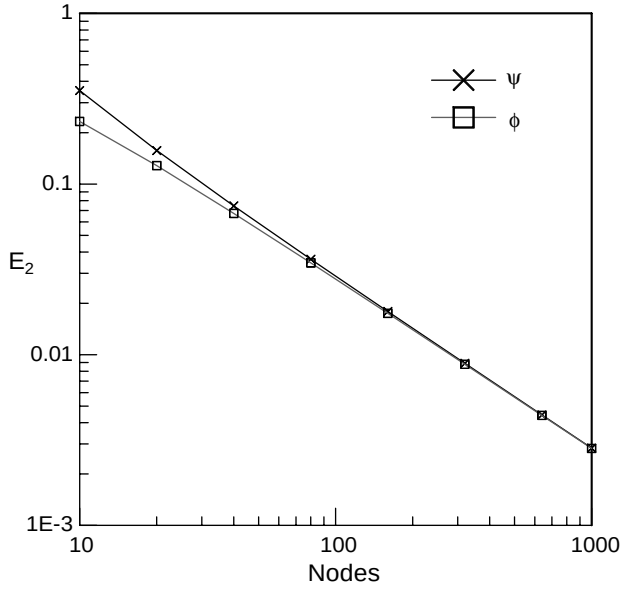

Fig. 6. Root-mean-square errors of the normal derivative of velocity potential (ϕ) and stream function (ψ).

4. Conclusions

After the desingularization of boundary integral equations and their normal derivative equations, the singular and hypersingular boundary integral equations become nonsingular. The comparison between several schemes is shown for their convergence and performance. Some important features of the normal derivative boundary integral equation are recognized. Although only a simple example is calculated, the characteristic of both types of integral formulations is still obtained.

In the Neumann problems, the boundary integral equation originally belongs to the Fredholm integral equation of the second kind. After taking the normal derivative on it, the modified equation becomes the Fredholm integral equation of the first kind with a hypersingular kernel. Even though the hypersingular equation can be reduced into two weakly singular integral equations, the results indicate that its convergence speed is only to $O(N^{-1})$, which is much less than the original singular boundary integral equation.

In the Dirichlet problems, the boundary integral equation belongs to the Fredholm integral equation of the first kind. After taking the normal derivative on it, the equation becomes the second-kind equation with a regular kernel. However, even though this is a second-kind equation with a regular kernel, its convergence speed is still only to $O(N^{-1})$, whereas the original singular equation converges to $O(N^{-3})$.

When both the boundary integral equation and its normal derivative are applied simultaneously, the error from the normal-derivative equation will be much higher than that from its original form. Denser grid points should be used for the normal-derivative integral equation, to maintain the same accuracy of computing. Overall, the desingularization of boundary integral equations does actually avoid the difficulties of the perplexing singularities for boundary integral equations. Though direct mathematical integration generally gives better accuracy but with more efforts and also limits to simple geometry. However, for more general cases, the desingularization formulation from the original singular boundary integral equations is recommended since proposed numerical method will give more accurate results as far as Neumann and Dirichlet problems are concerned.

Acknowledgements

The work in this paper was partially supported by the National Science Council, Taiwan under Grants No. NSC

89-2211-E-002-057 and NSC 89-2611-E-002-045. It is gratefully appreciated.

References

[1] Sladek V, Sladek J, editors. Singular integrals in boundary element methods. Boston: Computational Mechanics Publications; 1998.
[2] Hess JL, Smith AM. Calculation of nonlifting potential flow about arbitrary three-dimensional smooth bodies. J Ship Res 1964;7:22–44.
[3] Kantorovich LV, Krylov VI. Approximate methods for higher analysis. Interscience 1958.
[4] Landweber L, Macagno M. Irrotational flow about ship forms, Iowa: IIHR Report No. 123; 1969.
[5] Fan CM, Young DL. Analysis of the 2D stokes flows by the non-singular boundary integral equation method. Int Math J 2002;2: 1199–215.
[6] Webster WC. The flow about arbitrary, three-dimensional smooth bodies. J Ship Res 1975;19:206–18.
[7] Cao Y, Schultz WW, Beck RF. Three-dimensional desingularized boundary integral methods for potential problems. Int J Numer Methods Fluids 1991;12:785–803.
[8] Lalli F. On the accuracy of the desingularized boundary integral method in free surface flow problems. Int J Numer Methods Fluids 1997;25:1163–84.
[9] Zhang YL, Yeo KS, Khoo BC, Chong WK. Simulation of three-dimensional bubbles using desingularized boundary integral method. Int J Numer Methods Fluids 1999;31:1311–20.
[10] Chen W, Tanaka M. A meshless, exponential convergence, integration-free and boundary-only RBF technique. Comput Math Appl 2002;43:379–91.
[11] Hwang WS, Huang YY. Nonsingular direct formulation of boundary integral equations for potential flows. Int J Numer Methods Fluids 1998;26:627–35.
[12] Chuang JM. Numerical studies on desingularized Cauchy's formula with applications to interior potential problems. Int J Numer Methods Eng 1999;46:805–24.
[13] Hwang WS. Hypersingular boundary integral equation for exterior acoustic problems. J Acoust Soc Am 1997;101:3336–42.
[14] Yang SA. On the singularities of Green's formula and its normal derivative, with an application to surface-wave-body interaction problems. Int J Numer Methods Eng 2000;47:1841–64.
[15] Saranen J. The modified quadrature method for logarithmic-kernel integral equations on closed curves. J Integral Equations Appl 1991;3: 575–600.
[16] Chien CC, Rajiyah J, Atluri SN. An effective method for solving the hypersingular integral equations in 3-D acoustics. J Acoust Soc Am 1990;88:918–37.
[17] Lin Y, Rudolphi TJ. Some identities for fundamental solutions and their applications to weakly-singular boundary element formulations. Eng Anal Boundary Elem 1991;8:301–11.
[18] Okada H, Rajiyah J, Atluri SN. Non-hyper-singular integral-representations for velocity (displacement) gradients in elastic/plastic solids (small or finite deformations). Comput Mech 1989;4:165–75.
[19] Chien CC, Rajiyah J, Atluri SN. On the evaluation of hyper-singular integral arising in the boundary element method for linear elasticity. Comput Mech 1991;8:57–70.